



**HAL**  
open science

# Tailoring Spectral Properties of Binary PT-Symmetric Gratings by Duty-Cycle Methods

Anatole Lupu, H. Benisty, Andrei V. Lavrinenko

► **To cite this version:**

Anatole Lupu, H. Benisty, Andrei V. Lavrinenko. Tailoring Spectral Properties of Binary PT-Symmetric Gratings by Duty-Cycle Methods. *IEEE Journal of Selected Topics in Quantum Electronics*, 2016, 22 (5), pp.4402807. 10.1109/JSTQE.2016.2542791 . hal-01698888

**HAL Id: hal-01698888**

**<https://hal-iogs.archives-ouvertes.fr/hal-01698888>**

Submitted on 27 Nov 2019

**HAL** is a multi-disciplinary open access archive for the deposit and dissemination of scientific research documents, whether they are published or not. The documents may come from teaching and research institutions in France or abroad, or from public or private research centers.

L'archive ouverte pluridisciplinaire **HAL**, est destinée au dépôt et à la diffusion de documents scientifiques de niveau recherche, publiés ou non, émanant des établissements d'enseignement et de recherche français ou étrangers, des laboratoires publics ou privés.

# Tailoring spectral properties of binary PT-symmetric gratings by duty-cycle methods

A. Lupu, H. Benisty, and A. V. Lavrinenko

**Abstract**— We explore the frequency selective functionalities of a nonuniform PT-symmetric Bragg grating with modulated complex index profile. We start by assessing the possibility to achieve an efficient apodization of the PT-symmetric Bragg grating spectral response by using direct adaptations of the conventional apodization techniques. A particular emphasis is put on the binary type structures with different duty cycle variations. We subsequently propose a new efficient grating modulation technique allowing for largely improved reflection/transmission characteristics of the Bragg gratings. The overall intention of our approach is to adapt conventional Bragg gratings designs to improve a PT-symmetric case, fostering thus a new generation of active photonic devices.

**Index Terms**—Integrated optoelectronics, optical amplifiers, waveguides, coupled mode analysis, PT-symmetry.

## I. INTRODUCTION

The proposal in 1998 by Bender and Boettcher that the concept of respecting parity-time (PT) symmetry “non-Hermitian Hamiltonians” could stand as a complex extension of the conventional quantum mechanics quickly became a new paradigm in theoretical physics [1,2]. Adapting the concept in optics, the refractive index of PT symmetric structures is complex-valued with adequately incorporated gain and loss in spatially separated regions of the system. The spatial distributions of gain-loss can either occur in the direction transverse to the light propagation, as in the case of the coupled directional couplers, or along the light propagation direction, as in the case of the PT-symmetric Bragg gratings (PTBGs) shown in Fig. 1. Apart from fundamental research motivations, the interest in these artificial systems is strongly driven by the practical outcomes from two unique properties of PTBGs:

(i) Spatial (modal) non-reciprocity [3-9], different from that based on the Faraday magneto-optical effect. As illustrated in Fig. 1 the reflectivity of a PTBG can be extremely low for light incident from one side, and extremely high when light is

incident from the opposite side. This property can even be obtained without any gain by using a fully passive approach, provided that an appropriate amount of loss is incorporated in the system [10-12].

(ii) A large evolution of dispersion properties and band gap behavior of a PTBG induced by a limited variation of the gain-loss level [5,6]. Such dispersion changes can be advantageously exploited for implementing switches and modulators controlled by tuning of the gain-loss level [13-20].

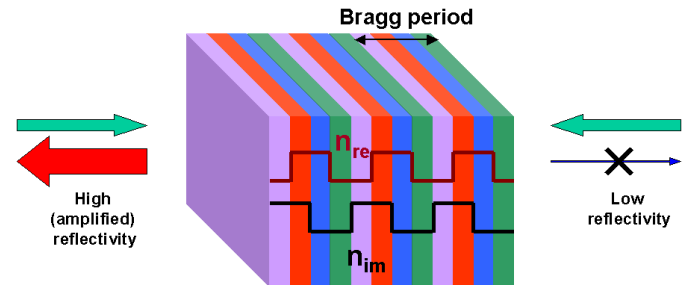


Fig. 1. Sketch of a PT-symmetric Bragg mirror and associated complex index profile  $n_{re} + in_{im}$ .

As was learnt over decades in the case of conventional passive type Bragg gratings with countless applications in optical networks, one of the most stringent requirements to be fulfilled for practical applications is related to the control of the spectral response and/or Bragg grating dispersion properties. For instance, the use of Bragg gratings as filters in Wavelength Division Multiplexing (WDM) requires the efficient control of the whole spectral shape, related namely to the reduction of the secondary sidelobes level. Such reduction is usually achieved by tapering the coupling strength profile, a process known as apodization. The implementation of apodization techniques regarding PT-symmetric systems has been to the best of our knowledge unexplored so far and this motivates the present work. A particular emphasis is put on the use of binary type structures and duty-cycle variation methods.

The paper is organized as follows. The generic case of PTBGs with tapering of the real and imaginary components of the refractive index profile thanks to conventional window apodization functions is treated in Section 2. Possible combinations for separate tapering of the real and imaginary components of the coupling profile are left for more detailed studies. Section 3 is dedicated to the tapering of the complex coupling profile by using duty cycle methods in the case of periodic binary structures. In Section 4 we compare the efficiency of this method with that of using modulated

Submitted for review 30 November 2015.

A. Lupu is with the Institut d’Electronique Fondamentale, CNRS, Univ Paris Sud, Université Paris-Saclay, 91405 Orsay, France (e-mail: anatole.lupu@u-psud.fr).

H. Benisty is with the Laboratoire Charles Fabry, Institut d’Optique Graduate School, CNRS, Univ Paris Sud, Université Paris-Saclay 2, Avenue Augustin Fresnel, 91127 Palaiseau Cedex, France (e-mail: henri.benisty@institutoptique.fr).

A. Lavrinenko is with DTU Fotonik – Department of Photonics Engineering, Technical University of Denmark, Oerstedts Plads 343, DK-2800 Kgs. Lyngby, Denmark (e-mail: alav@fotonik.dtu.dk).

aperiodic structures and propose a new modulation technique which leads to largely improved Bragg gratings characteristics. Conclusions end the paper.

## II. APODIZATION OF THE PT-SYMMETRIC BRAGG GRATING SPECTRAL RESPONSE BY TAPERING OF THE COMPLEX PROFILE

We consider a one-dimensional (1D) Bragg grating of length  $L$  with the PT-symmetric refractive index distribution,  $n(z) = n_0 + \Delta n_R(z) R(z) + i\Delta n_I(z) I(z)$  in the interval  $|z| < L/2$ . The system is embedded in a homogeneous medium having a uniform refractive index  $n_0 = 1.4$  for  $|z| > L/2$ . The considered case loosely corresponds to that of a Bragg grating written in an optical fiber. Here,  $\Delta n_{I,R}(z)$  represent the fast varying index contrast shifted by a  $\Lambda/4$  for the real and imaginary parts (e.g.  $\Delta n_R(z) \propto \cos(2\pi z/\Lambda)$  and  $\Delta n_I(z) \propto \sin(2\pi z/\Lambda)$  for a sinusoidal variation), while  $R(z)$ ,  $I(z)$  are the slowly varying tapered envelopes of the real and imaginary modulations of the refractive index, respectively. The fact that the index contrast here is two orders of magnitude larger than in a usual fiber grating does not affect the generality of obtained results and offers some computational advantages.

As known, in the case of conventional passive type gratings the shape of the spectral response follows the Fourier transform of the tapering function [21]. In our study we consider an example of the Hamming type apodization function  $f(z) = 1 + 0.852\cos(2\pi z/L)$  that is used as envelope for  $R(z)$  and  $I(z)$ . The Hamming apodization provides in conventional gratings an optimal suppression of the first sidelobes.

The resulting spectral response obtained for a 64 periods PTBG with index contrast  $\Delta n = \pm 0.02$  is displayed in Fig. 2(a). For the sake of comparison, the spectral response of a uniform PTBG is also presented as a reference. The application of the Hamming function envelope suppresses the sidelobes level by approximately 30 dB as compared to the unapodized grating spectral response. On the other hand the reflection level remains very low for both apodized and uniform PTBGs for the reversed direction of light propagation [Fig. 2(b)]. Note that the transmission level is practically not perturbed by the apodization procedure. The obtained results are totally consistent with the well defined roles of the factors in the apodized index profile:

$$n(z) = n_0 + f(z)\Delta n e^{i2\pi z/\Lambda} \quad (1)$$

The slow envelope  $f(z)$  brings spectral apodization while the complex single side-band modulation  $\Delta n \times \exp(i2\pi z/\Lambda)$  results in the non-reciprocal PT-symmetric behavior [3,4].

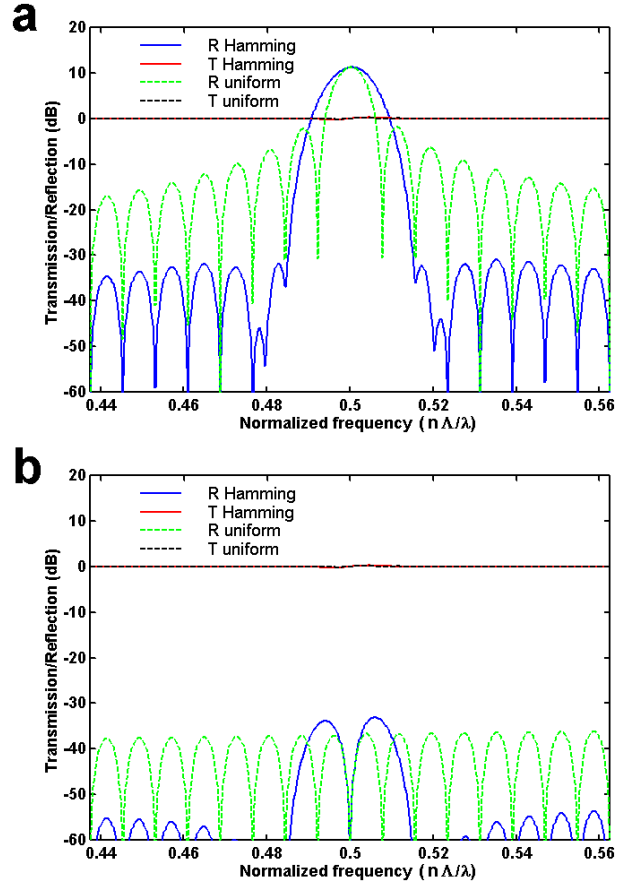


Fig. 2. (a) Reflection and transmission spectra of apodized and uniform PT-symmetric Bragg gratings for light injection from the front side; (b) Same for light injection from the end-side.

The apodization of spectral response with any window function features a larger index contrast in the middle of the grating with progressive reduction of the contrast toward the grating edges  $|z| = L/2$  to minimize the Gibbs phenomenon. Conversely, a modulation profile that is maximal at the edges of the grating and minimal in the center results in a strong increase of the sidelobes level, a rarely desired feature per se.

To summarize, the apparent situation is quite similar to that occurring for passive-type apodized Bragg gratings. One substantial difference, however, is that the complex index profile of the PT-symmetric Bragg grating brings an additional degree of freedom. It becomes possible to independently modulate the real and imaginary components of the index profile. It is thus interesting to consider a Bragg grating with a pseudo-PT symmetric index profile, where modulation of the real and imaginary index are only balanced on average, across the whole structure, but are not locally equal. On the single period scale, the modulations of the real and imaginary index being unbalanced, the grating is not locally PT-symmetric. But we will see that the distributed nature of the interaction nevertheless causes similar features in spite of this absence of rigorous (local and global) PT symmetry.

To illustrate the behavior of such pseudo PTBG we consider for  $R(z)$  and  $I(z)$  a pair of cosine functions superimposed onto the same constant modulation:

$$f(z) = 1 + A_{R,I} \cos(2\pi z / L) \quad (2)$$

where coefficients  $|A_{R,I}| < 1$  but may be distinct for the real and imaginary index modulations. Color maps corresponding to reflection and transmission spectra for the three fixed values of  $A_R = 0.852$ ;  $0$ ;  $-0.852$  and variable  $|A_I| < 1$  are shown in Figs. 3(a-c), respectively.

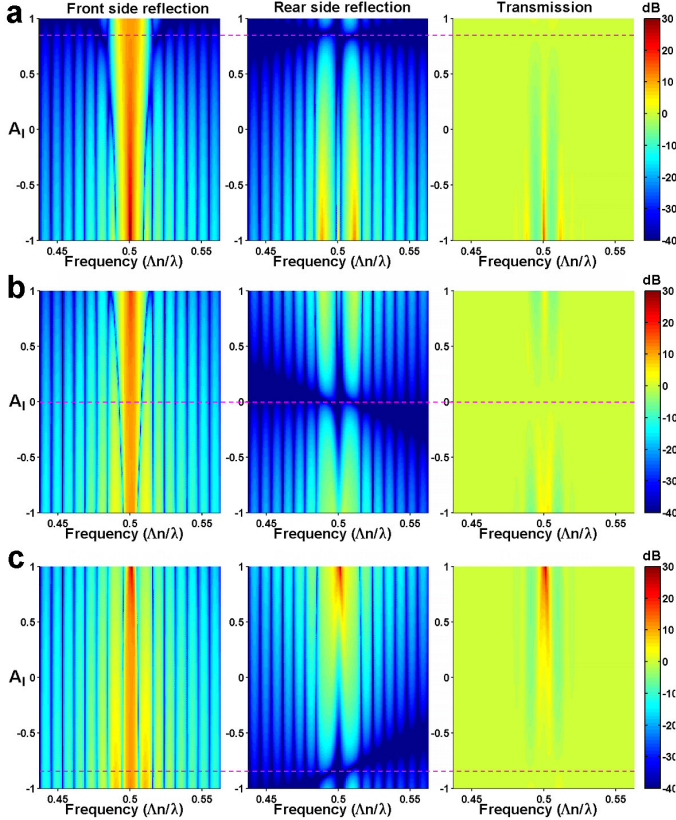


Fig. 3. Reflection and transmission spectra of pseudo PT-symmetric Bragg gratings as function of parameter  $A_I$  used for modulation of the imaginary part of the index profile. a)  $A_R = 0.852$ ; b)  $A_R = 0.0$ ; c)  $A_R = -0.852$ .

The three color maps in Fig. 3(a) illustrate the situation when the real part of the index profile is modulated with the Hamming function ( $A_R = 0.852$ ) and the imaginary part is modulated with variable  $A_I$ . The dotted line at  $A_I = 0.852$  indicates the case depicted above in Fig. 2 of the apodized PTBG. It can be seen that the degradation of the spectral response with deviation from the ideal situation when  $A_I = A_R$ , e.g. the re-emergence of sidelobes, is rather gradual. The tail suppression of the spectral response still remains acceptable for  $\pm 15\%$  variations around the optimal value of  $A_I = 0.852$  associated with the rigorous PT-symmetry. Furthermore, the non-reciprocal grating behavior is persistent in the whole range of the  $A_I$  parameter variation.

A distinctive behavior can be observed with  $A_I \approx -1$ , i.e. with anti-tapering of the imaginary profile, opposite to the enhanced modulation of the real part in the middle of the grating. This combination results in a narrow amplified single mode transmission by 25 dB while the rear side reflection level is lower by 15 dB. This regime can be used for the realization of a narrow-band single-mode amplifier.

The color maps in Fig. 3(b) illustrate the case of a Bragg grating with uniform modulation of the real part of the index profile (hence  $A_R = 0$  and  $f(z) = 1$ ). The dotted line at  $A_I = 0$  indicates the position of the rigorous PT-symmetric index profile. As for the previous case the PT-symmetric non-reciprocal grating behavior is manifested throughout the whole range  $-1 < A_I < 1$ .

The color maps in Fig. 3(c) correspond to the case  $A_R = -0.852$ . As explained above, this situation is not favorable for the spectral tail suppression. Meanwhile a distinct interesting behavior can be observed when  $A_I \approx 1$ . A higher modulation of the real part of the index profile towards the ends of the grating combined with enhanced modulation of the imaginary part in the middle of the grating results here in the selection at the Bragg wavelength of a single and narrow longitudinal mode with more than 30 dB reduction over satellites lobes. This regime is highly desirable for a single-mode Distributed-Feedback (DFB) laser.

The above examples illustrate some useful functionalities for optics applications that can be achieved by using PT-symmetric grating structures with nonuniform complex index profiles. However, the bottleneck point that could preclude the actual application of these concepts is related to the difficulty of the technological realization of modulated complex index profile gratings, with materials locally sampling all combined degrees of modulation  $R(z)$  and  $I(z)$  along the tapers. It would be way simpler to use a unique set of materials for high and low refractive index units as well as for gain and loss media. The conventional solution employed to solve this issue in the case of passive binary type periodic structures is to use duty-cycle modulation methods. We examine in the next Section how to modify them.

### III. DUTY-CYCLE MODULATION OF BINARY PT-SYMMETRIC GRATINGS

The essence of the duty-cycle variation method when applied to periodic binary type gratings with alternating regions of high and low effective indices is to use the dependence of the coupling strength on the grating duty-cycle. Since such method is compatible with a binary etching process (using for simplicity a constant etch depth), it is especially attractive when Bragg-like structures are realized by surface corrugation techniques as it is often the case for photonic crystals or similar 1D or 2D periodic structures. Several duty-cycle variations methods are described in literature [22-26]. The basic duty cycle (BDC) variation method introduced by Sakata [22] uses the coupling strength dependence on the grating duty cycle, i.e. the ratio of the grating ridge width  $(\Lambda + \Delta)/2$  to the grating period  $\Lambda$ , where  $\Delta/2$  represents the ridge extra length with respect to the half period length [Fig. 4(a)]. The ‘‘Phase Shifted Pair Gratings’’ method (PSPG) [23] alternates on a double grating period length ( $2\Lambda$ ) ridges of length  $(\Lambda + \Delta)/2$  and  $(\Lambda - \Delta)/2$  separated by fixed  $\Lambda/2$  groove intervals [Fig. 4(b)], resulting in two cells of unequal length within the  $2\Lambda$  period. The off-resonance modulation (ORM) method [24,25] is based on alternating whole gratings cells



(ridge+groove) of modulated lengths  $\Lambda+\Delta$  and  $\Lambda-\Delta$  [Fig. 4(c)]. Finally, the concatenated gratings method (CG) proposed by Wiessman [26] represented in Fig. 4(d) is similar to the ORM with the difference that grating cells are of length  $\Lambda-\Delta$  and  $\Delta$ , truly retaining period  $\Lambda$ . The comparative analysis of different duty-cycle variation methods requires a separate discussion, which is not the scope of the present paper. Here, we focus our attention on the BDC and ORM methods that can be considered as the two most generic methods for coupling strength modulation in the case of periodic and deterministically aperiodic gratings, respectively (in their simplest form).

The mean value  $\chi_i$  of the coupling coefficient for the  $i$ -th grating cell is proportional to the amplitude of the main harmonics when the grating coupling profile is decomposed in a Fourier series. In the case of the BDC modulation, there is one cell per period (the grating period is constant) and the first term of the Fourier series is given by the expression:

$$\chi_{BDC} \sim \frac{1}{\pi} \sin\left(\frac{\pi(\Lambda+\Delta)}{2\Lambda}\right) = \frac{1}{\pi} \cos\left(\frac{\pi\epsilon}{2}\right) \quad (3)$$

Here  $\epsilon=\Delta/\Lambda$  is the  $i$ -th grating cell relative variation of the high or low index sections lengths, i.e. the groove/ridge asymmetry. By convention we associate  $\epsilon$  with the high index grating section length variation. For window apodization functions, the modulation  $\epsilon$  is maximal (no groove) at the edges of the grating, where the coupling strength vanishes, and gradually decreases toward the middle of the grating, where the coupling strength is maximal (symmetric grating).

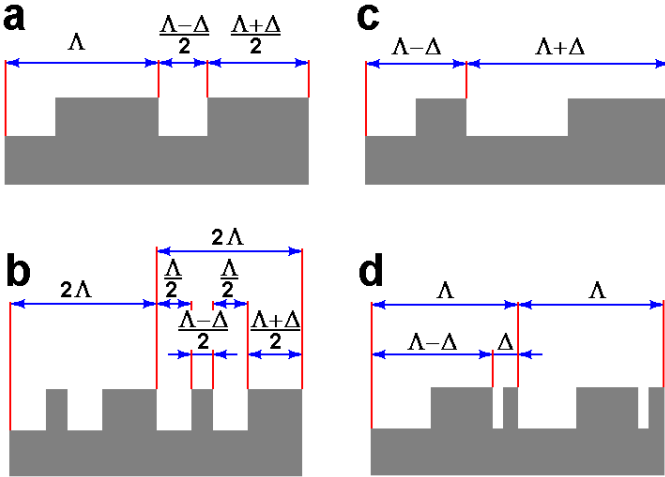


Fig. 4. Duty-cycle modulation methods: (a) Basic Duty-Cycle variation (BDC); (b) Phase-Shifted Pair Gratings (PSPG) method, of actual period  $2\Lambda$ ; (c) Off-resonance Modulation (ORM) method, with two compensating cells of unequal period within a  $2\Lambda$  periodic pattern; (d) The similar Concatenated Grating (CG) method variant, where the period is  $\Lambda$ , and  $\Delta$  has a different meaning.

Since in the case of the BDC method, in contrast with the uniform PTGB [Fig. 5(a)], the length of the grating section with high index  $n_H$  differs from that of the section with low index  $n_L$ , the immediate question is how then the binary variation of the imaginary part of the index profile could be

implemented? From general considerations, it is quite clear that in order to maintain PT-symmetric behavior the average level of gain and loss should remain balanced. To answer this question we consider the following example of a BDC modulated grating, where for heuristic reasons the grating period  $\Lambda$  and modulation strength  $\epsilon$  are constant.

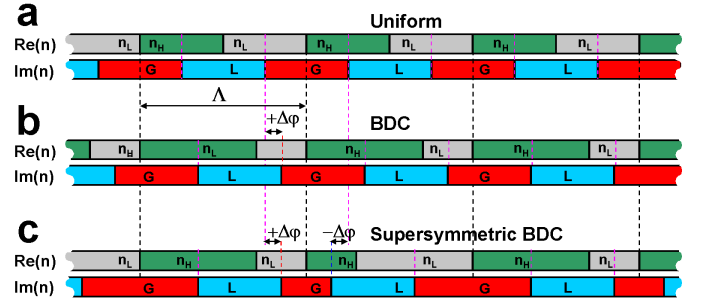


Fig. 5. Schematic of PT-symmetric binary gratings. a) Uniform; b) BDC; c) Supersymmetric BDC. The black dotted indicate cell boundaries, while magenta dotted lines - low and high index point at half-sections boundaries, where the Gain/Loss (G/L) boundaries are then defined.

One solution depicted in Fig. 5(b) is to implement an alternation of gain (G) and loss (L) according to the following algorithm: each high and low index sections are divided in two halves and gain (loss) is then assigned to the adjacent  $n_H$   $n_L$  half-sections. Such a procedure automatically ensures the conservation of gain-loss balance along the grating.

To verify the validity and efficiency of such a method, we consider the example of linear (triangular) modulation:

$$\mathcal{E}(z) \propto C_m \left| (z - L/2) / L \right| \quad (4)$$

where  $C_m = \max(\epsilon_i)$  quantifies the maximal relative grating section length variation.

The color maps in Fig. 6(a) illustrate the spectral response resulting from such a modulation of the complex index profile. The dotted line at  $C_m = 0$  indicates the position of the rigorous PT-symmetric index profile. It can be seen that the tail suppression of the spectral response is by far less efficient as compared to the case of the Hamming type profile [Fig. 3(a)]. Furthermore, a marked drift of the spectral response central wavelength as a function of modulation strength  $C_m$  is observed. Such a drift of the central length as a function of the duty-cycle modulation is inherent and intrinsic to the BDC method and is not related to the PT-symmetric aspect of the problem [27]. Meanwhile, the PT-symmetric behavior of the grating is also affected. This is clearly evident from the transmission spectrum color map when  $|C_m| \approx 1$ . In contrast to the case of a PTBG apodized with the Hamming function that was represented in Fig. 2, the transmission of the BDC apodized binary grating is amplified by around 6 dB. The origin of such a discrepancy stems from the fact that the grating duty-cycle modulation with the BDC method also alters the PT-symmetric complex index profile. Upon inspection of Fig. 6(b) it can be observed that the modulation of the imaginary part of the index profile results in an additional phase shift  $-\Delta\phi$  with respect to that of a uniform

PT-symmetric Bragg grating. Consequently the phase shift between the real and imaginary parts of the index profiles becomes locally different from  $\pi/2$  required by rigorous PT-symmetry.

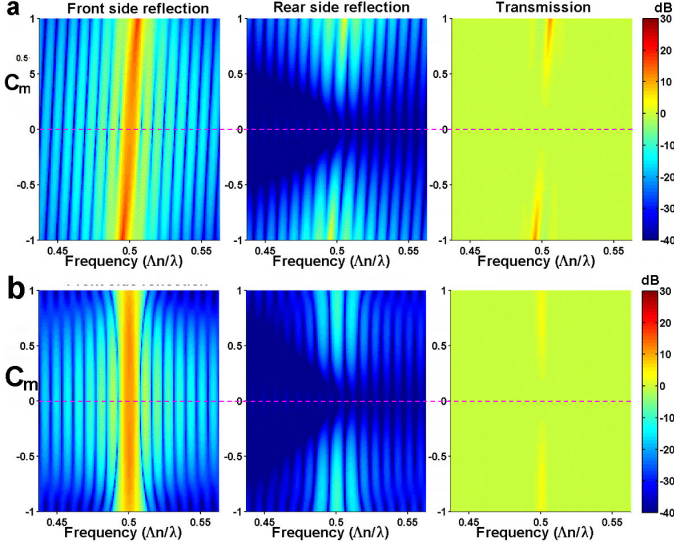


Fig. 6. Reflection and transmission spectra of binary PT-symmetric Bragg gratings as function of duty cycle modulation parameter  $C_m$ . a) BDC modulation method; b) supersymmetric BDC modulation method.

To solve this issue and improve the performances of the BDC method we consider the "supersymmetric" approach represented in Fig. 5(c). Instead of the periodicity rule it is based on a mirror inversion of a given cell while defining the adjacent one. In this case the additional phase shift of the imaginary profile  $+\Delta\phi$  of one cell is compensated by the phase shift  $-\Delta\phi$  of the adjacent cell resulting in a net zero shift for two consecutive cells. The period is then  $2\Lambda$ . The color maps in Fig. 6(b) illustrate the spectral response resulting from such "supersymmetric" BDC method. It can be seen that the tail suppression of the spectral response is greatly improved in two respects. Suppression of the secondary sidelobes by  $\sim 23$  dB with respect to the main lobe level at the central wavelength is achieved for modulation strength  $|C_m| \approx 0.7$ . Furthermore, the above mentioned drift of the central wavelength is also suppressed.

Nevertheless, despite the marked improvement of performances, they are still below those obtained with the Hamming apodization function, prompting more analysis. Upon inspection of Fig. 5(c) it can be observed that the modulation of the gain/loss sequence occurs only for one type of section. In our case only the length of gain sections is modulated while that of loss sections remains always the same. This is at variance with the  $n_H/n_L$  sequence, where both low and high index section lengths are modulated. In accordance with Eq. (3) this means that the grating strength for the real and imaginary parts of the grating profile is modulated by a different amount. So we constrained the phase shift to the proper value but lost the proper amplitude. The solution to solve this issue is to consider a different type of modulation scheme, where, instead of the duty cycle, the local period of cells of the grating is changed. This is the essence of

the ORM method proposed in [24,25], which can be considered as a first step toward deterministic aperiodic binary systems.

#### IV. DETERMINISTIC APERIODIC BINARY PT-SYMMETRIC GRATINGS

For our analysis we consider the example of an ORM grating. In contrast to the BDC method the duty cycle is the same for every grating cell. It is the cell length that varies along the grating. In order to find the variation of the grating coupling strength it is necessary to consider two consecutive cells forming a genuine period:

$$\Lambda_i = \Lambda + \Delta \quad \text{and} \quad \Lambda_{i+1} = \Lambda - \Delta \quad (5)$$

As represented in Fig. 4(c)  $\Lambda$  is the period (cell) length for a uniform grating and  $\Delta$  is the added cell-to-cell modulation. By analogy with the BDC method the local grating modulation ratio can be defined as:

$$\varepsilon_i = \Delta_i / 2\Lambda \quad (6)$$

The mean coupling coefficient obtained through straightforward calculation for one period (two cells) is then:

$$\chi_{ORM} \sim \frac{1}{\pi} \left( 1 + \cos \left( \frac{\pi \Delta}{\Lambda} \right) \right) = \frac{1}{\pi} \cos^2 \left( \frac{\pi \varepsilon}{2} \right) \quad (7)$$

Since for ORM it is only the period that varies but the  $n_H/n_L$  duty-cycle remains fixed, the extension of this method to the PT-symmetric case is straightforward. As shown in Fig. 7(b) for each grating period the PT-symmetric profile is introduced absolutely in the same manner as for a uniform grating [Fig. 7(a)], i.e., with borders of the imaginary part sections pegged at the centers of the real part ones.

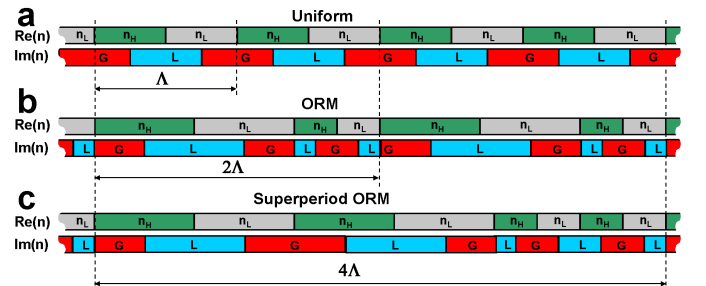


Fig. 7. Schematic of PT-symmetric binary gratings. a) Uniform; b) BDC; c) Supersymmetric BDC. The black dotted indicates one period boundaries.

To verify the efficiency of the ORM approach, we consider again the example of linear modulation described by Eq. (4). The color maps in Fig. 8(a) illustrate the spectral response obtained with the ORM method. It is basically very similar to that obtained with the supersymmetric BDC method with only a marginal improvement. This is due to the fact that there is still an important asymmetry in the modulation of the imaginary part of the index profile. In the considered case the

length of the loss sections locally experiences a stronger modulation as compared to the length of the gain sections.

To solve this issue and improve performances of the ORM method we employ again a supersymmetric version as in Fig. 7(c), which now doubles the period from  $2\Lambda$  to  $4\Lambda$ . One could be more general, and introduce a superperiodic grating structure having more replica with proper symmetries but we can check that the impact of one  $2\Lambda$  replica is already satisfying here. The color maps in Fig. 8(b) illustrate the spectral response obtained with the  $4\Lambda$  “superperiodic” ORM gratings (SORM). The tail suppression of the spectral response is greatly improved, most clearly around the appearing “nodal valleys”.

A more detailed view of the spectral response corresponding to the case of modulation strength  $|C_m| \approx 0.5$  is provided in Fig. 9(a), this value being that of the tilted nodal “valleys” in the front side reflection panel from Fig. 8(b). The secondary sidelobes are suppressed by  $\sim 27$  dB with respect to the main lobe level in the center. Furthermore, the rear side reflection level is also much lower. The transmission is also very close to that of the uniform or Hamming apodized PTBG. With respect to all parameters the PT-symmetric grating behavior is practically totally restored, and the tolerances of structural parameters are large.

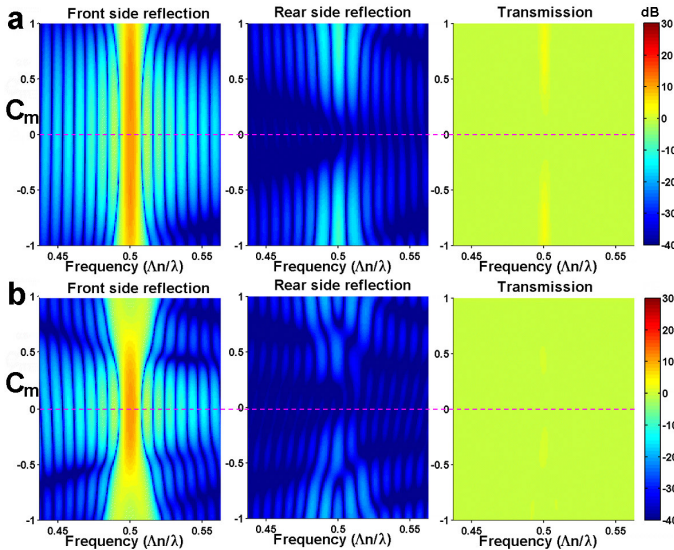


Fig. 8. Reflection and transmission spectra of binary PT-symmetric Bragg gratings as function of grating period modulation parameter  $C_m$ . a) ORM method; b) supersymmetric ORM method. The dotted line at  $C_m = 0$  indicates the position of the rigorous PT-symmetric index profile.

These are not, indeed, the only advantages of the SORM method. As shown in Fig. 9(b), a qualitatively different flat-hat behavior can be achieved when the modulation strength is  $|C_m| \approx 0.7$ , because we see in Fig. 8(b) (left panel) that the central ridge splits in two broad crests for  $|C_m| > 0.75$ . Such kind of flat-hat behavior is highly desirable in many WDM applications with modern data formats. While it is naturally obtained with passive Bragg grating structures, it is not the case for their standard PT-symmetric counterparts. The “superperiodic” ORM thus allows restoring this highly desirable feature.

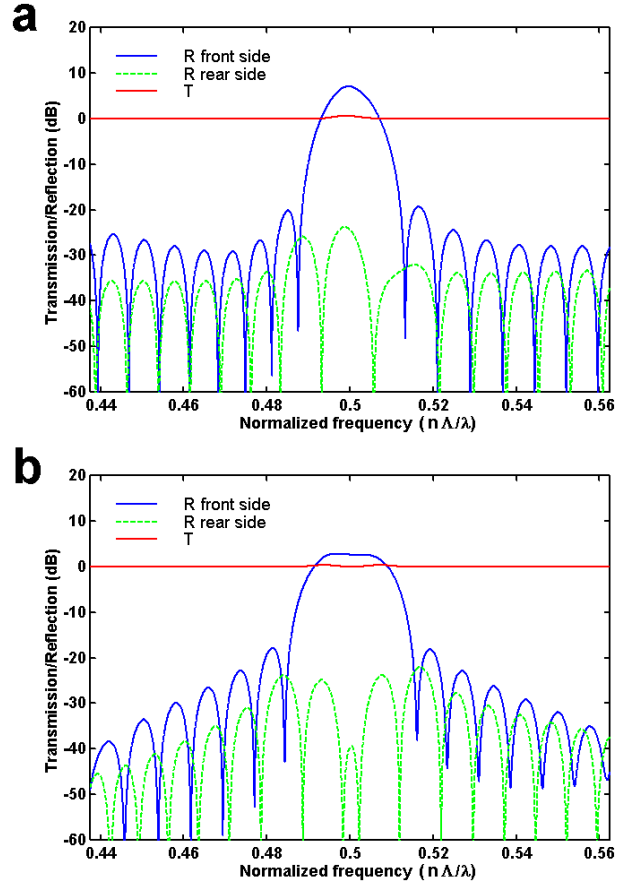


Fig. 9. Reflection and transmission spectra of SORM apodized binary PT-symmetric Bragg gratings. Grating modulation modulation strength a)  $|C_m| \approx 0.5$ ; b)  $|C_m| \approx 0.7$ .

## V. CONCLUSION

In the presented work we considered nonuniform PT-symmetric Bragg gratings with a complex index profile modulated by a slowly varying envelope function, with the aim of combining the apodization techniques of classical Bragg gratings with the advantages of PT-symmetry such as unidirectionality. We demonstrated the possibility to achieve an efficient apodization of the PT-symmetric Bragg grating spectral response with a standard Hamming window function. To ease implementation of the apodization in real structure with local binary nature of the real and imaginary index contributions, this approach was extended to the duty-cycle modulated periodic or deterministic aperiodic binary PT-symmetric gratings. The analysis leads us to propose a new efficient grating modulation technique labeled as the superperiodic off-resonance modulation method (referred as SORM). The undertaken approach demonstrates that many conventional techniques previously developed for passive type Bragg gratings or related devices can be transposed and adapted to a PT-symmetric case, provided the constraints of real and imaginary part modulation are properly combined. This approach indicates a likely perspective for fostering a new generation of active photonic devices.



## REFERENCES

- [1] C. M. Bender and S. Boettcher, "Real spectra in non-Hermitian Hamiltonians having PT-symmetry," *Phys. Rev. Lett.* 80, 5243 (1998).
- [2] C. M. Bender, "Making sense of non-Hermitian Hamiltonians," *Rep. Prog. Phys.* 70, 947–1018 (2007).
- [3] L. Poladian, "Resonance mode expansions and exact solutions for nonuniform gratings," *Phys. Rev. E* 54, 2963–2975 (1996).
- [4] M. Greenberg and M. Orenstein, "Irreversible coupling by use of dissipative optics," *Opt. Lett.* 29, 451–453 (2004).
- [5] M. Kulishov, J. M. Laniel, N. Bélanger, J. Azaña, and D. V. Plant, "Nonreciprocal waveguide Bragg gratings," *Opt. Express* 13, 3068–3078 (2005).
- [6] Z. Lin, H. Ramezani, T. Eichelkraut, T. Kottos, H. Cao, and D. N. Christodoulides, "Unidirectional invisibility induced by PT-symmetric periodic structures," *Phys. Rev. Lett.* 106, 213901–4 (2011).
- [7] Y. D. Chong, Li Ge, and A. Douglas Stone, "PT-Symmetry Breaking and Laser-Absorber Modes in Optical Scattering Systems," *Phys. Rev. Lett.* 106, 093902 (2012).
- [8] A. Mostafazadeh, "Invisibility and PT symmetry," *Phys. Rev. A* 87, 012103–8 (2013).
- [9] H. F. Jones, "Analytic results for a PT-symmetric optical structure," *J. Phys. A* 45, 135306 (2012).
- [10] L. Feng, M. Ayache, J. Huang, Y. -L. Xu, M. -H. Lu, Y. -F. Chen, Y. Fainman, and A. Scherer, "Nonreciprocal light propagation in a silicon photonic circuit," *Science* 333, 729–733 (2011).
- [11] L. Feng, Y.-L. Xu, W. S. Fegadolli, M.-H. Lu, J. E. Oliveira, V. R. Almeida, Y.-F. Chen, and A. Scherer, "Experimental demonstration of a unidirectional reflectionless parity-time metamaterial at optical frequencies," *Nat. Mater.* 12, 108–113 (2012).
- [12] M. Kulishov and B. Kress, "Free space diffraction on active gratings with balanced phase and gain/loss modulations," *Opt. Express* 20, 29319–29328 (2012).
- [13] L. Feng, X. Zhu, S. Yang, H. Zhu, P. Zhang, X. Yin, Y. Wang, and X. Zhang, "Demonstration of a large-scale optical exceptional point structure," *Opt. Express* 22, 1760–1767 (2014).
- [14] A. Lupu, H. Benisty, and A. Degiron, "Using optical PT symmetry for switching applications," *Photonics Nanostruct.:Fundam. Appl.* 12, 305–311 (2014).
- [15] S. Phang, A. Vukovic, H. Susanto, T. M. Benson, and P. Sewell, "Ultrafast optical switching using parity-time symmetric Bragg gratings," *J. Opt. Soc. Am. B* 30, 2984–2991 (2013).
- [16] S. Phang, A. Vukovic, H. Susanto, T. M. Benson, and P. Sewell, "Impact of dispersive and saturable gain/loss on bistability of nonlinear parity-time Bragg gratings," *Opt. Lett.* 39, 2603–2606 (2014).
- [17] S. Phang, A. Vukovic, H. Susanto, T. M. Benson, and P. Sewell, "A versatile all-optical parity-time signal processing device using a Bragg grating induced using positive and negative Kerr-nonlinearity," *Optical and Quantum Electronics* 47, 37–47 (2014).
- [18] M. Kulishov, H. F. Jones, and B. Kress, "Analysis of PT -symmetric volume gratings beyond the paraxial approximation," *Opt. Express* 23, 9347–9362 (2015).
- [19] S. V. Suchkov, A. A. Sukhorukov, J. Huang, S. V. Dmitriev, C. Lee and Y. S. Kivshar, "Nonlinear switching and solitons in PT-symmetric photonic systems" *Laser & Photonics Reviews*, vol. 10 pp.177–213, 2016.
- [20] C. Hahn, S. H. Song, C. H. Oh, P. Berini, "Single-Mode Lasers and Parity-Time Symmetry Broken Gratings Based on Active Dielectric-Loaded Long-Range Surface Plasmon Polariton Waveguides," *Opt. Express* 23, 19922–19931 (2015).
- [21] H. Kogelnik, "Filter response of non-uniform almost-periodic structures," *Bell System Technical Journal*, 55, 109–126 (1976).
- [22] H. Sakata, "Sidelobe suppression in grating-assisted wavelength-selective couplers," *Opt. Lett.*, vol. 17, 463–465 (1992).
- [23] D.-B. Kim, C.-Y. Park, B.-H. O, H.-M. Kim, T.-H. Yoon, "Fabrication of sidelobe-suppressed InP-InGaAsP vertical-coupler optical filter using pair grating structure", *IEEE Photonic Technology Letters* 10, 1593–1595 (1998).
- [24] A. Lupu, A. Carencu, "Grating-type optical filter with apodised spectral response," patent WO 2000002078 A1, 01/07/1998; patent US 6549707 B1.
- [25] A. Lupu, A. Carencu, P. Win, H. Sik, P. Boulet, M. Carre, and S. Slempek, "Spectral response apodization of Bragglike optical filters," in *Optical Fiber Communication Conference (OFC)/International Conference on Integrated Optics and Optical Fiber Communications* (IOOC), Postconference Digest (Optical Society of America, Washington, D.C., 1999), paper WM26-7, pp. 271–273.
- [26] D. Wiesmann, C. David, R. Germann, D. Emi, G.L. Bonna, "Apodized surface-corrugated gratings with varying duty cycles," *IEEE Photonic Technology Letters* 12, 639–641 (2000).
- [27] A. Lupu, "Wavelength demultiplexers for the optical access network," PhD thesis N°:99 PA11 2204, Université de Paris 11, Orsay, FRANCE (1999).

## Biographies



**Anatole Lupu** received the M.S., degrees from the Moscow Engineering Physics Institute in 1985 and Ph.D., Dr. Hab. From Paris Sud University, Orsay, France, in 1999 and 2008, respectively. He is a tenured CNRS scientist with twenty five years research activity in optoelectronics performed both in academic and industrial labs (Moscow Lebedev Physics Institute, Technical

University of Moldova, CNET/France Telecom, Corning Inc.). He joined Institut d'Electronique Fondamentale (IEF) in 2003. Since 2012 he is the head of the Photonic Crystals and Metamaterials group at IEF. His current research interests are dealing with the theoretical and experimental studies in the areas of metamaterials, nanophotonics, plasmonics and PT-symmetric devices. He published, in total, circa 100 research papers and holds 5 patents.



**Henri Benisty** received the Ph.D. degree from University Paris 6, Paris, France, in 1989, on accumulation layers at Si interfaces. His research topics have been first nanostructure growth and physics (Thomson, Orsay) and lamellar III–VI compounds (Paris 6 University, Paris, France).

Since 1994, he has been involved in research on microcavities (mainly for LEDs) and in photonic crystals in two dimensions on III–V semiconductors in laboratory PMC, Palaiseau, France. He was with University of Versailles and he is with the Laboratoire Charles Fabry, Institut d'Optique Graduate School, Palaiseau Cedex, France. He coordinated the EU project "FUNFOX" on photonic crystal functional integrated circuits. He currently investigates applications of periodic nanostructures to LEDs, biophotonics, fluorescence based or label-free in UV, various blocks of miniature photonic integrated circuits and multimode structures, and novel plasmonic hybrid waveguides. He cofounded the biochip-related start-up Genewave, Paris, France (now merged with Mobidiag, Finland).



**Andrei V. Lavrinenko** received the M.S., Ph.D., and D.Sci. degrees from the



Belarussian State University (BSU), Minsk, Belarus, in 1982, 1989, and 2004, respectively. He was an Assistant Professor and Associate Professor with the Physics Department, BSU, from 1990 to 2004. Since 2004, he has been an Associate Professor with the Department of Photonics Engineering of the Technical University of Denmark. Since 2008, he has been leading the Metamaterials Group of this department. He is the author or co-author of more than 400 publications, including 5 textbooks, 9 book chapters and more than 140 journal papers. His research interests are in metamaterials, plasmonics,

photonic crystals, quasicrystals and photonic circuits, slow light, and numerical methods in electromagnetics and photonics.